SSRG International Journal of Thermal Engineering
ISSN: 2395-0250/ https://doi.org/10.14445/23950250/IJTE-V9I1P102

Volume 9 Issue 1, 12-24, Jan-Apr 2023

Original Article

Magnetic Field as Vibration Attenuator for Slightly Curved Branched Carbon Nanotubes in a Thermal-Nanofluidic Environment

Yinusa Ahmed[1] and Sobamowo Gbeminiyi[2]

[1,2]*Mechanical Engineering Department, University of Lagos, Nigeria.*

Received: 27 February 2023 Revised: 02 April 2023 Accepted: 18 April 2023 Published: 30 April 2023

Abstract *- This present study presents distinctive models that capture the nonlinear longitudinal and transverse vibrations of branched, slightly curved embedded nanotubes that convey nanofluids and operate in thermal-magnetic environments. Euler beam equation and Hamilton and Erigen's theorems are employed for the development of the system's governing equations of motion. Subsequently, these equations are solved with the aid of PDE tools and PDE solvers MATLAB. The solutions obtained via the employment of these tools are used for parametric study and visualization after proper and adequate verification and validation. From the results, it is obvious that an augmentation in the branched angle increases the nanotube's instability. Besides, the magnetic term attenuates the vibrations of the slightly curved branched nanotubes by over 20%. It is anticipated that the outcomes of this present study will give improved insights into the vibration analyses of straight and branched nanotubes that rest on elastic foundations and operate in thermal-magnetic and thermal-nanofluidic environments.*

Keywords *- Branched nanotubes, Magnetic field, PDE-tools, Stability, Vibration attenuation.*

1. Introduction

After the publication of the finding of nanotubes in microtubule forms, different studies on branched Nanostructures have been investigated (Terrones et al., 2002). This is a result of their excellent performance when employed for the purpose of nanosensors, transistors and diodes (Chernozatonskii, 1992). In an attempt to correlate the review of past work using real-life constraints, the pipe-walking occurrences presented by Olunloyo et al. (2010) were considered. Şimşek et al. (2011) performed critical investigations on nano-terms' influences on force vibrations of coupled nanotubes with internally flowing nanoparticles and recorded the variation between the nonlocal and classical approaches. They also stressed the need for nonlocal approaches for dynamic and stability analyses.

Meanwhile, the impacts of thermal terms on vibrations of embedded nanotubes using arbitrary boundary conditions have been presented by Ansari et al. (2011). Rafiei et al. (2012) obtained stability results for flow-induced vibrations in nanotubes embedded in viscoelastic foundations in another research work. Subsequently, Liang and Su (2013) made available avenues for exploring the impacts of nonlocal parameters on viscous fluid conveying nanotubes by generating stability plots using the frequency ratios and mean flow velocities in the nanotubes. The nonlocal effects on the nanotube's stability were then explicitly illustrated and discussed. Askari et al. (2014) scrutinized nonlinear vibrations of nanotubes under thermal influences and embedded in nonlinear elastic foundations. The nonlinear foundation was considered to approximate to foundation better than the linear equivalent. The obtained thermal impacts on frequency responses for the different radii of SWCNT are then to establish the impact of thermal on the stability of the CNT. Belhadj et al. (2017) used a reduced equation of motion to analyse the vibration of an SWCNT using a nonlocal approach. They employed a semi-analytical technique and obtained results for both stability and steady-state responses of the simply supported SWCNT considered in the research. The dimensional frequency model obtained in the study was also varied with the effective length of the CNT for the first three modes. They realized that an augmentation in the mode number considerably increases the dimensionless frequency for the same length of CNT. Bijan et al. (2018) scrutinized the nonlinear vibrations of viscous flow-induced vibrations TWNT that is embedded in a Pasternak foundation. The influences of amplitude and nonlinear Pasternak foundation coefficient on the frequency ratio of the CNT are also explained. The work further explains how a negligible assumption on the Knudsen number could give a different value of the critical velocity of the viscous fluid flowing through the CNT. Eltaher and

Mohamed (2020) considered the unforced vibration of perfect and imperfect carbon nanotubes under pre-buckling and post-buckling loads. During the analysis, they were able to obtain non-dimensional buckling loads for the first three modes and for two different boundary conditions.

Recently, Sobamowo, Akanmu and Adeleye et al. (2021) presented comprehensive thermo-mechanical and magneto-geometric parameters effects on the dynamic behaviour of multi-walled CNT resting on an elastic foundation. They employed a semi-analytical scheme known as the Perturbation method with Homotopy (HPM) to solve the developed governing equation. The work went further to present results for the CNT's steady state and dynamic responses. It established that an intensification in dimensionless amplitude resulted in a corresponding increase in CNT dimensionless frequency ratio. Other recent works that employ modeling have been presented by Abubakar et al. (2020), Sami (2020), Simon et al. (2020), Yash (2022) and Sami (2022). As previously presented, various studies have been put forward to predict and analyze the behaviour of fluid-conveying CNTs in several ways. Previous works have neglected a collective study that discussed how magnetic fields could be used to attenuate the vibration of slightly curved nanotubes in various thermal-mechanical environments. Such needs serious attention for proper analysis of the fluid–conveying CNT. Consequently, in this work, a Nonlinear Vibration Analysis of an Embedded Slightly Curved Branched Fluid-conveying CNT Operating in a Magnetic Environment is presented and analyzed using numerical approaches.

2. Methodology and Governing Equations

2.1. CNTs with Different Branch Angles

Consider the schematic of straight and branched fluid conveying nanotubes resting on an elastic foundation in a thermal-magnetic environment, as in Figure 1. The different shapes formed are also depicted in Table 1 and Figure 1.

2.2. Development of Governing Equations for Nonlinear Coupled Flow Induced Vibration

Several variational methods may be employed to derive the governing differential equations of an elastic body. The minimum energy potential principle, minimum complementary energy, and stationary Reissner energy may be employed to formulate static problems. The variational principle that is valid for the dynamics of systems of particles, rigid bodies, or deformable solids is called Hamilton's principle, where the variation of the function is taken with respect to time. Consider an SWCNT conveying fluid subjected to the magnetic field and supported with linear and nonlinear elastic foundations (Winkler and Pasternak foundations), as shown in Figure 1. Applying the Nonlocal-Eringen's theory of elasticity, Euler Bernoulli's theory for beams and variational Hamilton's principle, the equations of motion and boundary conditions can be derived. Starting with Hamilton's principle, which can be illustrated: (Yinusa et al., 2019, Yinusa et al., 2020, Yinusa et al., 2021, Yinusa et al., 2022)

$$\int_0^t \left(\delta u_T - \delta k_T - \delta \mathrm{v}_T\right) dt = 0, \tag{1}$$

The strain energy variation of the CNT is simply

$$\delta u_T = \frac{1}{2}\iiint_{V_t} \sigma_{xx}\delta\varepsilon_{xx} dV_t = \frac{1}{2}\int_0^L \int_{A_t} \sigma_{xx}\delta\varepsilon_{xx} dx dA_t, \tag{2}$$

but $\varepsilon_{xx} = -zw''$, substitute into (1) and simplify to obtain:

$$\delta u_T = \frac{1}{2}\int_0^L \left[M_{xx}\nabla^2\left(\delta w\right)\right] dx. \tag{3}$$

Similarly, the variation of kinetic energy and virtual work done by the CNT is obtained as:

$$\delta k_T = \begin{pmatrix} \frac{1}{2}\int_0^L \int_{A_t} \rho_t \left[\left(\frac{\partial(\delta\tilde{u})}{\partial t}\right)^2 + \left(\frac{\partial(\delta\tilde{w})}{\partial t}\right)^2 \right] dx dA_t \\ + \frac{1}{2}\int_0^L \int_{A_t^f} \rho_t^f \delta\left[(\Gamma U)^2 + \left(\frac{\partial w}{\partial t} + \Gamma U \frac{\partial w}{\partial x}\right)^2 \right] dx dA_t^f \\ + \frac{1}{2}\int_0^L m_j \delta\left(\delta(x-L)\left[\left(\frac{\partial\tilde{u}}{\partial t}\right)^2 + \left(\frac{\partial\tilde{w}}{\partial t}\right)^2 \right]\right) dx \\ \frac{1}{2}\int_0^L m_j^f \delta\left[(\Gamma U)^2 + \left(\frac{\partial w}{\partial t} + \Gamma U \frac{\partial w}{\partial x}\right)^2 \right] \delta(x-L)\, dx \end{pmatrix} and$$

$$\delta v_T = \int_0^L \begin{pmatrix} \mu_{eff} A_t^{vf} \nabla^2 \left(\frac{\partial w}{\partial t} + \Gamma U \frac{\partial w}{\partial x}\right) + \left(\begin{matrix} M_f (\Gamma U)^2 [1-\cos\phi] \\ + PA - T - K_P - \frac{EA\alpha\Delta\theta}{1-2\nu} \end{matrix}\right) \frac{\partial^2 w}{\partial x^2} \\ + \left[\frac{B_o^2 \cos^2\alpha A_t}{\mu_p}\right] \nabla^2 w - \left[\frac{B_o^2 \sin^2\alpha I^{CNT}}{\mu_p}\right] \nabla^4 w \\ - \sigma B_o^2 \cos^2\alpha A_f \left(\frac{\partial w}{\partial t} + \Gamma U \frac{\partial w}{\partial x}\right) + k_w w + k_3 w^3 - G\frac{\partial^2 w}{\partial x^2} + c\frac{\partial w}{\partial t} \end{pmatrix} \delta w dx. \tag{4}$$

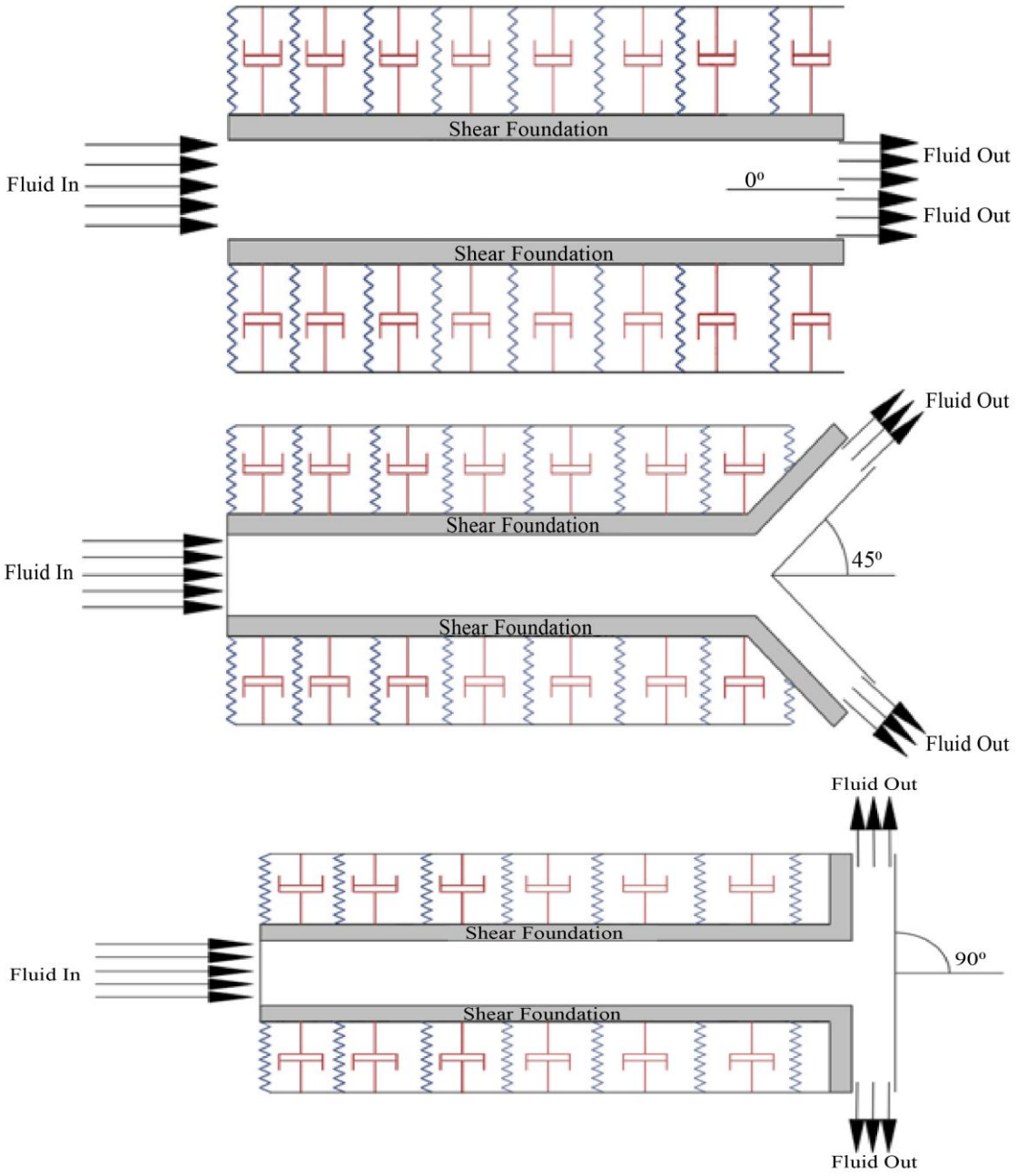

Fig. 1 Different shapes of CNTs

Table 1. CNTs with different branched angles

Downstream angle (ϕ^o)	Shape of CNT
0	I shape
15	Sharp Y Shape
30	Sharp Y Shape
45	Y Shape
60	Slack Y Shape
75	Slack Y Shape
$75 < \phi < 90$	T Shape

Substitute Equations 3 and 4 into Equation 1, integrating by part and setting the coefficient δw to zero, gives the longitudinal and transverse vibration equations for a fluid conveying carbon nanotube (CNT) as:

$$
\begin{aligned}
&m\ddot{u}_1 + 2m_f\Gamma U\dot{u}_1'' + m_f\Gamma\dot{U}u_1''' + m_f\Gamma\ddot{U} + m_f\Gamma^2UU'(1+u_1') + [T_0 - G - EA_t]w_1'w_1'' - (EA_t - m_f\Gamma^2U^2)u_1'' + (PA)'(1-2\nu\delta) - PA(1-2\nu\delta)w_1'w_1''\\
&-EA_t'\left(u_1' + \frac{1}{2}w_1'^2\right) - \frac{(PA)'}{2}(1-2\nu\delta)w_1'^2 + E\alpha(A\Delta T' + A'\Delta T) - \frac{E\alpha}{2}w_1'^2(A\Delta T' + A'\Delta T) - E\alpha A\Delta Tw_1'w_1'' - EI\left(w_1^{iv}w_1' + w_1''w_1'''\right)\\
&+(e_oa)^2\left[\begin{array}{l}
m\ddot{u}_1'' + 2\Gamma m_f\left(U''\dot{u}_1'' + 2U'\dot{u}_1''' + U\dot{u}_1^{iv}\right) + \Gamma m_f\left(\dot{U}''u_1''' + 2\dot{U}'\dot{u}_1^{iv} + \dot{U}\dot{u}_1^{v}\right) + \Gamma m_f\ddot{U}'' + \Gamma^{-2}m_f\begin{pmatrix}3U'U''(1+u') + 2U'^2u_1'' + UU'''(1+u_1')\\ +2UU''u_1'' + UU'u_1'''\end{pmatrix}\\
+\begin{pmatrix}(T_0 - G - EA_t)w_1'w_1^{iv} + 3(T_0 - G - EA_t)w_1''w_1'''\\ -2EA_t'w_1'w_1''' - 2EA_t'w_1''^2 - EA_t''w_1'w_1''\end{pmatrix} + \left(\begin{pmatrix}EA_t'' - 2\Gamma^2m_fU'^2\\ -2\Gamma^2m_fUU''\end{pmatrix}u_1'' + 2\left(EA_t' - 2m_f\Gamma^2UU'\right)u_1''' + \left(EA_t - m_f\Gamma^2U^2\right)u_1^{iv}\right)\\
+(1-2\nu\delta)\left(P'''A + 3P''A' + 3P'A'' + PA'''\right) + (1-2\nu\delta)\begin{pmatrix}P''Aw_1'w_1'' + 2P'A'w_1'w_1'' + 2P'Aw_1''^2 + 2P'Aw_1'w_1''' + PA''w_1'w_1'' + 2PA'w_1''^2\\ +2PA'w_1'w_1''' + 3PAw_1''w_1''' + PAw_1'w_1^{iv}\end{pmatrix}\\
+E\left(A_t'''\left(u_1' + \frac{1}{2}w_1'^2\right) + 2A_t''\left(u_1'' + w_1'w_1''\right) + A_t'\left(u_1''' + w_1''^2 + w_1'w_1'''\right)\right) + \frac{1}{2}(1-2\nu\delta)\begin{pmatrix}(P'''A + 3P''A' + 3P'A''w_1'w_1'' + PA'''w_1'w_1''')w_1'^2\\ +(4P''A + 2P'A' + PA'')w_1''w_1'\\ +2(P'A + PA')w_1''^2 + (P'A + PA')w_1'''\end{pmatrix}\\
+E\alpha\left(3A''\Delta T' + 3A'\Delta T'' + A\Delta T''' + A'''\Delta T\right) + \frac{E\alpha}{2}\begin{pmatrix}\begin{pmatrix}3A''\Delta T' + 3A'\Delta T''\\ +A\Delta T''' + A'''\Delta T\end{pmatrix}w_1'^2 + 4\left(2A'\Delta T' + A\Delta T'' + A''\Delta T\right)w_1'w_1''\\ +2(A\Delta T' + A'\Delta T)w_1''^2 + 2(A\Delta T' + A'\Delta T)w_1'w_1'''\end{pmatrix}\\
+E\left(\alpha\begin{pmatrix}A''\Delta Tw_1'w_1'' + 2A'\Delta T'w_1'w_1'' + 2A'\Delta Tw_1''^2 + 2A'\Delta Tw_1'w_1''' + A\Delta T''w_1'w_1'' + 2A\Delta T'w_1''^2\\ +2A\Delta T'w_1'w_1''' + 3A\Delta Tw_1''w_1''' + A\Delta Tw_1'w_1^{iv}\end{pmatrix} + EI\left(w_1^{vi}w_1' + 3w_1^{v}w_1'' + 4w_1^{iv}w_1'''\right)\right)
\end{array}\right] = F_1(x,t) + (e_oa)^2\frac{\partial^2F_1(x,t)}{\partial x^2}
\end{aligned}
\tag{5}
$$

$$
\begin{aligned}
&m\ddot{w}_1 + \left(c + A_f\sigma B_o^2\cos^2\varphi\right)\dot{w}_1 + 2m_f\Gamma U\dot{w}_1' + m_f\Gamma\dot{U}w_1' + m_f\Gamma^2UU'w_1' - \left[T_0 - P(1-2\nu\delta)A - G - k_p - m_f\Gamma^2U^2\cos\phi - \frac{B_o^2\cos^2\varphi}{\mu_p}\right]w_1'' + \left[T_0 - P(1-2\nu\delta)A - G - EA\right]\left[w_1'u_1'' + w_1''u_1' + \frac{3}{2}w_1'^2w_1''\right]\\
&+P(1-2\nu\delta)Aw_1'\left(1 - u_1' - \frac{1}{2}w_1'^2\right) - EA\left[w_1'u_1' + \frac{1}{2}w_1'^3\right] + E\alpha A\Delta Tw_1'\left(1 - u_1' - \frac{1}{2}w_1'^2\right) + E\alpha A\Delta T'\left(1 - u_1' - \frac{1}{2}w_1'^2\right) + E\alpha A'\Delta Tw_1'\left(1 - u_1' - \frac{1}{2}w_1'^2\right) - E\alpha A\Delta Tw_1'\left(u_1'' + w_1'w_1''\right) + \left(EI + \frac{IB_o^2\sin^2\varphi}{\mu_p}\right)w_1^{iv}\\
&-EI\left(3u_1'''w_1'' + 4u_1''w_1''' + 2u_1'w_1^{iv} + w_1'u_1^{iv} + 2w_1'^2w_1^{iv} + 8w_1'w_1''w_1''' + 2w_1'^4\right) - \frac{EA}{L}\int_0^L\left(z_0'w_1' + \frac{1}{2}w_1'^2\right)dx\left[w_1'' + z_0''\right] + k_1w_1 + k_2w_1^3
\end{aligned}
$$

$$
\begin{aligned}
&\left\{\begin{array}{l}
m\ddot{w}_1'' + \left(c + A_f\sigma B_o^2\cos^2\varphi\right)\dot{w}_1'' + 2\Gamma m_f\left(U''\dot{w}_1' + 2U'\dot{w}_1'' + U\dot{w}_1'''\right) + \Gamma m_f\left(\dot{U}''w_1' + 2\dot{U}'w_1'' + \dot{U}w_1'''\right) + \Gamma^2m_f\left(3U''U'w_1' + 2U'^2w_1'' + UU'''w_1' + 2UU''w_1'' + UU'w_1'''\right)\\
-\begin{pmatrix}T_0 - G - k_p\\ -\frac{B_o^2\cos^2\varphi}{\mu_p}\end{pmatrix}w_1^{iv} + (1-2\nu\delta)\begin{pmatrix}P''Aw_1''\\ +2P'A'w_1''\\ +2P'Aw_1'''\\ +PA''w_1''\\ +2PA'w_1'''\\ +PAw_1^{iv}\end{pmatrix} + m_f\Gamma^2\cos\phi\begin{pmatrix}2U'^2w_1''\\ +4UU'w_1'''\\ +2UU''w_1''\\ +U^2w_1^{iv}\end{pmatrix} + \begin{pmatrix}-\left(\frac{3}{2}w_1''w_1'^2 + U'w_1'' + U''w_1'\right)\left((-2\nu\delta P + E + P)A'' - (2\nu\delta - 1)(P''A + 2P'A')\right)\\ -2(-2\nu\delta P + E + P)A' + 4P'A\left(\nu\delta - \frac{1}{2}\right)\left(\frac{3}{2}w_1'^2 + U'\right)w_1''' + 3w_1'w_1''^2 + w_1'U'''\\ +2w_1''U'' + \left((2\nu\delta P - E - P)A - G + T_o\right)\left(\frac{3}{2}w_1'^2 + U'\right)w_1^{iv} + w_1'U^{iv}\\ +\left(9w_1'w_1'' + 3U''\right)w_1''' + 3w_1''^3 + 3w_1'U'''\end{pmatrix}\\
+(2\nu\delta - 1)\begin{pmatrix}AP\left(\frac{3}{2}w_1'^2 + U' - 1\right)w_1''' + APw_1'U''' + 3APw_1'w_1''^2 + \left(2APU'' + 2(P'A + PA')\left(\frac{3}{2}w_1'^2 + U' - 1\right)\right)w_1''\\ +w'P\left(\frac{1}{2}w'^2 + U' - 1\right)A'' + A\left(\frac{3}{2}w'^2 + U' - 1\right)P'' + (2P'A + 2PA')U'' + 2A'\left(\frac{1}{2}w'^2 + U' - 1\right)P'\end{pmatrix} - E\begin{pmatrix}Aw_1'''U' + 2Aw_1'U'' + 2A'w_1''U'\\ +Aw_1'U + 2A'w_1'U'' + A''w_1'U' +\\ \frac{1}{2}A''w_1'^3 + 3A'w_1'^2w'' + 3Aw_1'w_1''^2\\ +\frac{3}{2}Aw_1'^2w_1'''\end{pmatrix}\\
+(e_oa)^2\left\{\begin{array}{l}
+E\alpha\begin{pmatrix}A''\Delta T\left(1 - u_1' - 1/2w_1'^2\right)w_1' + 2A'\Delta T'\left(1 - u_1' - 1/2w'^2\right)w_1'\\ +2A'\Delta T\left(-u_1'' - w_1'w_1''\right)w_1' + 2A'\Delta T\left(1 - u_1' - 1/2w_1'^2\right)w_1''\\ +A\Delta T''\left(1 - u_1' - 1/2w_1'^2\right)w_1' + 2A\Delta T'\left(-u_1'' - w_1'w_1''\right)w_1'\\ +2A\Delta T'\left(1 - u_1' - 1/2w_1'^2\right)w_1'' + A\Delta T\left(-u_1'' - w_1''^2 - w_1'w_1'''\right)w_1'\\ +2A\Delta T\left(-u_1'' - w_1'w_1''\right)w_1'' + A\Delta T\left(1 - u_1' - 1/2w_1'^2\right)w_1'''\end{pmatrix} + \begin{pmatrix}\begin{pmatrix}-P''(-2\delta v + 1)A - 2P'(-2\delta v + 1)A'\\ -P(-2\delta v + 1)A'' - EA''\end{pmatrix}\left(w_1'u_1'' + w_1''u_1' + 3/2w_1'^2w_1''\right)\\ +2\left(-P'(-2\delta v + 1)A - P(-2\delta v + 1)A' - EA'\right)\begin{pmatrix}2w_1''u_1'' + w_1'u_1''' + w_1'''u_1'\\ +3w_1'w_1''^2 + 3/2w_1'^2w_1'''\end{pmatrix}\\ +\left(T_o - P(-2\delta v + 1)A - G - EA\right)\begin{pmatrix}3w_1'''u_1'' + 3w_1''u_1''' + w_1'u_1^{iv} + w_1^{iv}u_1'\\ +3w_1''^3 + 9w_1'w_1''w_1''' + 3/2w_1'^2w_1^{iv}\end{pmatrix}\end{pmatrix} + \left(\begin{matrix}EI +\\ \frac{IB_o^2\sin^2\varphi}{\mu_p}\end{matrix}\right)w^{vi}\\
+E\alpha\begin{pmatrix}\begin{pmatrix}A''\Delta T\left(1 - u_1' - 1/2w_1'^2\right)\\ +2A'\Delta T''\left(1 - u_1' - 1/2w_1'^2\right)\\ +2A'\Delta T'\left(-u_1'' - w_1'w_1''\right)\\ +2A'\Delta T'\left(1 - u_1' - 1/2w_1'^2\right)\\ +A\Delta T'''\left(1 - u_1' - 1/2w_1'^2\right)\\ +2A\Delta T''\left(-u_1'' - w_1'w_1''\right)\\ +2A\Delta T''\left(1 - u_1' - 1/2w_1'^2\right)\\ +A\Delta T'\left(-u_1'' - w_1''^2 - w_1'w_1'''\right)\\ +2A\Delta T'\left(-u_1'' - w_1'w_1''\right)\\ +A\Delta T'\left(1 - u_1' - 1/2w_1'^2\right)\end{pmatrix} + \begin{pmatrix}A'''\Delta T\left(1 - u_1' - 1/2w_1'^2\right)w_1'\\ +2A''\Delta T'\left(1 - u_1' - 1/2w_1'^2\right)w_1'\\ +2A''\Delta T\left(-u_1'' - w_1'w_1''\right)w_1'\\ +2A''\Delta T\left(1 - u_1' - 1/2w_1'^2\right)w_1''\\ +A'\Delta T''\left(1 - u_1' - 1/2w_1'^2\right)w_1'\\ +2A'\Delta T'\left(-u_1'' - w_1'w_1''\right)w_1'\\ +2A'\Delta T'\left(1 - u_1' - 1/2w_1'^2\right)w_1''\\ +A'\Delta T\left(-u_1'' - w_1''^2 - w_1'w_1'''\right)w_1'\\ +2A'\Delta T\left(-u_1'' - w_1'w_1''\right)w_1''\\ +A'\Delta T\left(1 - u_1' - 1/2w_1'^2\right)w_1'''\end{pmatrix} + \begin{pmatrix}A''\Delta T\left(u_1'' + w_1'w_1''\right)w_1'\\ +2A'\Delta T'\left(u_1'' + w_1'w_1''\right)w_1'\\ +2A'\Delta T\left(u_1''' + w_1''^2 + w_1'w_1'''\right)w_1'\\ +2A'\Delta T\left(u_1'' + w_1'w_1''\right)w_1''\\ +A\Delta T''\left(u_1'' + w_1'w_1''\right)w_1'\\ +2A\Delta T'\left(u_1''' + w_1''^2 + w_1'w_1'''\right)w_1'\\ +2A\Delta T'\left(u_1'' + w_1'w_1''\right)w_1''\\ +A\Delta T\left(u_1^{iv} + 3w_1''w_1''' + w_1'w_1^{iv}\right)w_1'\\ +2A\Delta T\left(u_1''' + w_1''^2 + w_1'w_1'''\right)w_1''\\ +A\Delta T\left(u_1'' + w_1'w_1''\right)w_1'''\end{pmatrix}\right) + EI\begin{pmatrix}5u_1^{v}w_1'' + 11u_1^{iv}w_1''' + 13u_1'''w_1^{iv} + 8u_1''w_1^{v}\\ +2u_1'w_1^{vi} + w_1'u_1^{vi} + 26w_1''^2w_1^{iv} + 16w_1'w_1^{v}w_1''\\ +28w_1'w_1^{iv}w_1''' + 2w_1'^2w_1^{vi} + 36w_1''w_1'''^2\end{pmatrix}\\
+\frac{EA}{L}\int_0^L\left(z'w_1' + \left(\frac{1}{2}w_1'\right)^2\right)dx\left(w_1^{iv} + z_0^{iv}\right) + 2\frac{EA'}{L}\int_0^L\left(z'w_1' + \left(\frac{1}{2}w_1'\right)^2\right)dx\left(w_1''' + z_0'''\right) + \frac{EA''}{L}\int_0^L\left(z'w_1' + \left(\frac{1}{2}w_1'\right)^2\right)dx\left(w_1'' + z_0''\right) + k_1w_1'' + k_2\left(3w_1'w_1'^2 + 6w_1w_1'^2\right)
\end{array}\right\} = F_1(x,t) + (e_oa)^2\frac{\partial^2F_1(x,t)}{\partial x^2}
\end{aligned}
\tag{6}
$$

The system's initial conditions are given as follows;

$$w(\tau=0)=a=A\cos\varpi\tau \qquad \dot{w}(\tau=0)=0 \tag{7}$$

While the B.C for steady-state analysis are;

Clamped at both ends

$$w\big|_{s=0}=0, \quad w'\big|_{s=0}=0 \qquad w\big|_{s=l}=0, \quad w'\big|_{s=l}=0 \tag{8}$$

Clamped-free (Cantilever)

$$w\big|_{s=0}=0, \quad w'\big|_{s=0}=0 \qquad w''\big|_{s=l}=0, \quad w'''\big|_{s=l}=0 \tag{9}$$

Pinned at both ends

$$w\big|_{s=0}=0, \quad w''\big|_{s=0}=0 \qquad w\big|_{s=l}=0, \quad w''\big|_{s=l}=0 \tag{10}$$

Clamped-pinned

$$w\big|_{s=0}=0, \quad w'\big|_{s=0}=0 \qquad w\big|_{s=l}=0, \quad w''\big|_{s=l}=0 \tag{11}$$

3. Vibration Solutions, Characteristic Equations and Eigenvalues

The research work presents equations of motion that capture transverse and longitudinal vibrations coupled with bulk thermal-fluidic variables, deformation and pressure variation. However, it is assumed that the deformation, thermal-fluidic and pressure models are annulled during simulation. Afterwards, PDE tools and PDE solvers in MATLAB are used on the outcome of the imposed assumptions. With the help of the numerical solutions, parametric studies were performed. For the sake of Stability analyses which will be carried out by employing bifurcation and phase-plane plots, the natural frequency is obtained using the boundary conditions from the resulting vibration solutions. The resulting equations are arranged in matrix form, as illustrated below;

$$\begin{bmatrix} \Gamma_{11}(\omega,\beta,\psi,e_0a,Ha,z,k,EI,...) & \Gamma_{12}(\omega,\beta,\psi,e_0a,Ha,z,k,EI,...) \\ \Gamma_{21}(\omega,\beta,\psi,e_0a,Ha,z,k,EI,...) & \Gamma_{22}(\omega,\beta,\psi,e_0a,Ha,z,k,EI,...) \end{bmatrix} \begin{bmatrix} \Lambda_1 \\ \Lambda_2 \end{bmatrix} = \begin{bmatrix} F_1^{BC} \\ F_2^{BC} \end{bmatrix} \tag{12}$$

When the determinant of the matrix is conditioned to varnish, the resulting equation is referred to as the characteristic equation of vibration. This equation is then solved to ascertain the system's natural frequency for any boundary condition considered (Yinusa *et al*., 2021, Yinusa *et al*., 2022). For the purpose of qualitative analysis, the vibration solution is mapped into a phase plane-dependent variable ***q(w, u, t)*** which is a function of *w, u* and *t.* This variable takes the form;

$$q(t)=\sum_{\xi=0}^{N} q_\xi t^\xi , \tag{13}$$

The combination of Equation 8 and its first derivative in time will then be used for the phase-plane qualitative stability analysis.

4. Results and Discussion

A parametric study is performed on developing MATLAB and MAPLE codes for the flow-induced vibrations in the nanotubes. Bifurcations and Qualitative stabilities in the tubes are first analyzed. Afterwards, the responses are presented, analyzed and discussed.

4.1. Influences of Branch Angles on Nanotube's Stability

Figure (2) and Figure (3) portray the influences of the branch angles on the nanotube's stabilities for pre- and post-bifurcations linear and nonlinear analyses. It is seen that the dimensionless frequency first decreases parabolically for increasing flow velocities for both linear and nonlinear foundations, implying that the CNT is stable in this domain. Beyond this domain, U_c is attained, and the vibration of the CNT turns unstable due to bifurcation. The implication of U_c is in the domain of 2.70 to 3.20 when considering linear analyses, and 4.20 to 5.16 for nonlinear implies that the system stabilizes better when the nonlinear model is applied. Furthermore, increasing the velocity of flow causing vibration results in U_s beyond which divergence or flutter may occur.

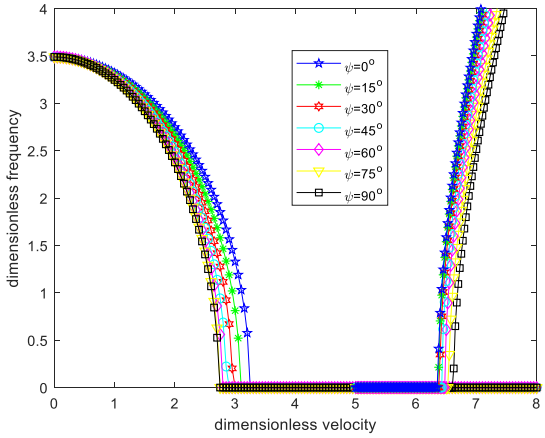

Fig. 2 Influences of branch angle on nanotube's stability For linear pre and post-bifurcation

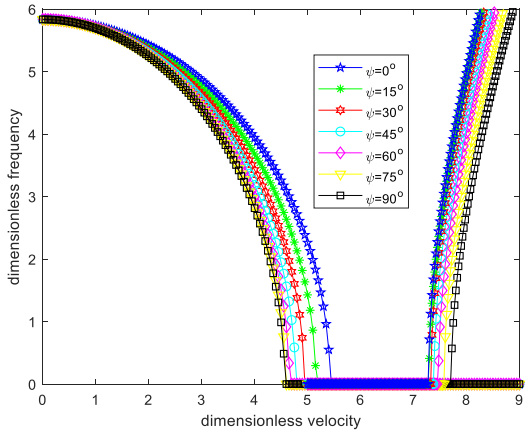

Fig. 3 Influences of branch angle on nanotube's stability For Nonlinear pre and post-bifurcation

4.2. Phase-Plane Plots of the Nanotube's Stability

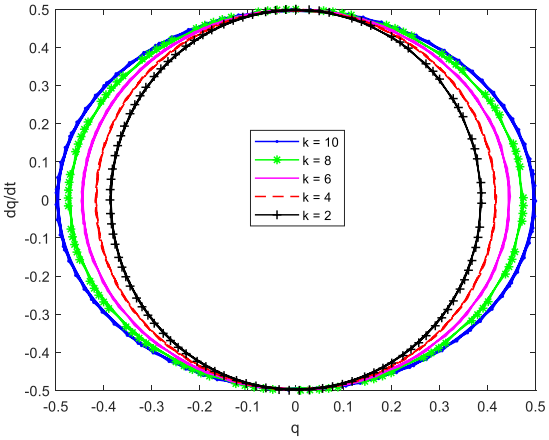

Fig. 4 Foundation effect for B = 0

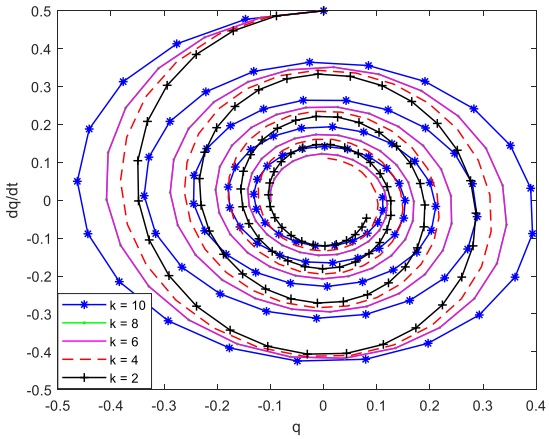

Fig. 5 Foundation effect for B = 10

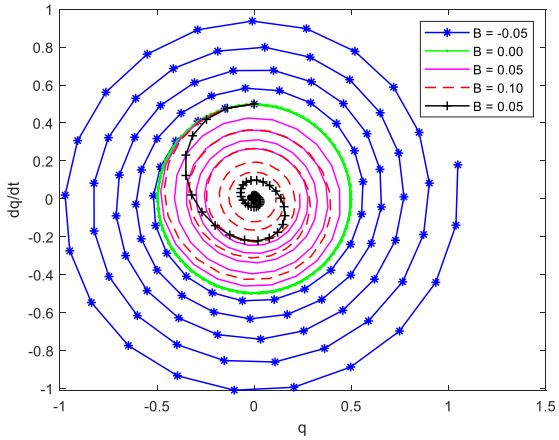

Fig. 6 Phase-plane with small negative damping

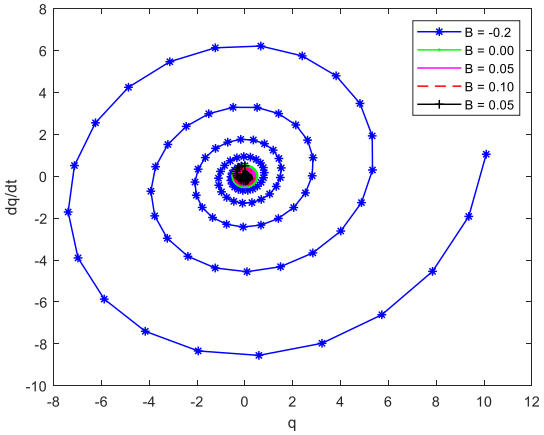

Fig. 7 Phase-plane with large negative damping

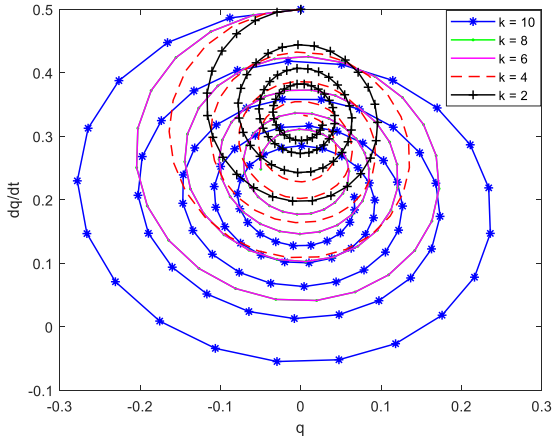

Fig. 8 Foundation effect on forced vibration with damping

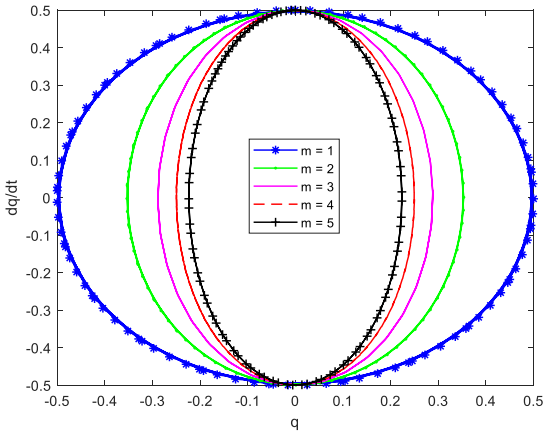

Fig. 9 Mass effect on MWCNT stability

Figure (4), Figure (5), Figure (6), Figure (7), Figure (8) and Figure (4) show the qualitative stability of the vibrating CNT. The complex part of the Eigenvalues obtained denote frequency, while the real part means damping. The fact that the obtained frequency is complex is the reason for the oscillation and vibration of the CNT under investigation. Neutral stability of CNT for nonlinear and linear vibration cases is first obtained. The vibration for these cases is about a fixed point called the center. There corresponding oscillations are also noticed and recorded appropriately. Subsequently, the impacts of the foundation parameter and magnetic field on the stability of the CNT are demonstrated in Figure 4 and Figure 5. An increase in foundation term increases the CNT stiffness and consequently results in a corresponding increase in the system's frequency in the absence of a magnetic field. However, the system's stability changes from neutral stability into a node or stable attractive immediately after the magnetic term is invoked. This further demonstrates the attenuating impact of the magnetic term as the solution curves move closer to the center. The impact of the magnetic field on the dynamic instability of the CNT is demonstrated using Figure 6 and figure 7. For $B \geq 0$ the vibrating system is stable due to the positive attenuating impact demonstrated by the magnetic field. The system loses its stability for the positive real part of the Eigenvalue solution, which corresponds to the negative damping influence from the magnetic field. This phenomenon occurs during resonance and should be chiefly avoided in design. The effect of foundation on forced vibration with damping is illustrated in Figure 8. The forced vibration with positive damping basically results in the system's oscillation with shifting centers. The effect of CNT mass on stability is shown in Figure 9 for neutral stability. The mass of the CNT possesses an antonymous effect as the system's stiffness. As the mass value is augmented, the vibration frequency reduces, as demonstrated in Figure 9.

Additionally, the phenomena of beats along the vibration history with and without magnetic influence are also studied. This occurs when the tube vibrates at close frequencies with another structure. The frequency of vibration of the beat system without magnetic effect is more than that with a magnetic field because the number of cycles completed is higher for the same time span.

4.3. Visualization of CNT Dynamic Response for Different Downstream Angles without Magnetic Field

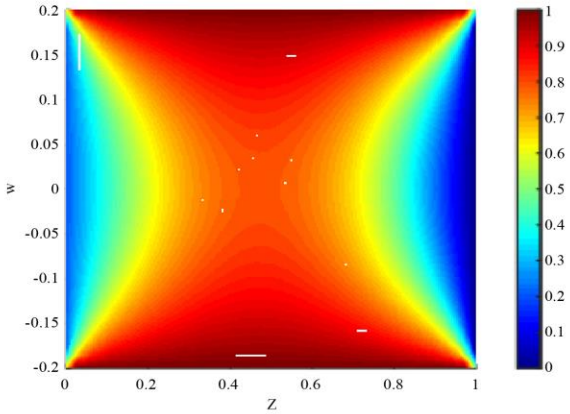

Fig. 10 CNT Deflection for φ = 0º

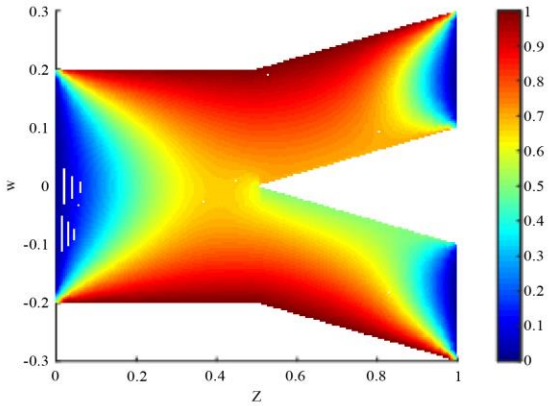

Fig. 11 CNT Deflection for φ = 30º

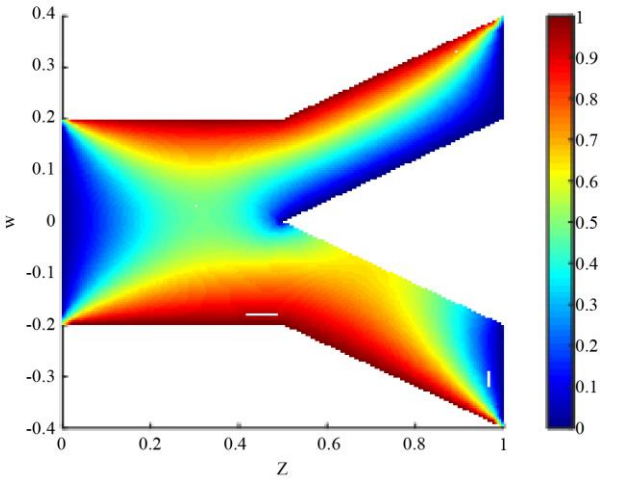

Fig. 12 CNT Deflection for φ = 45º

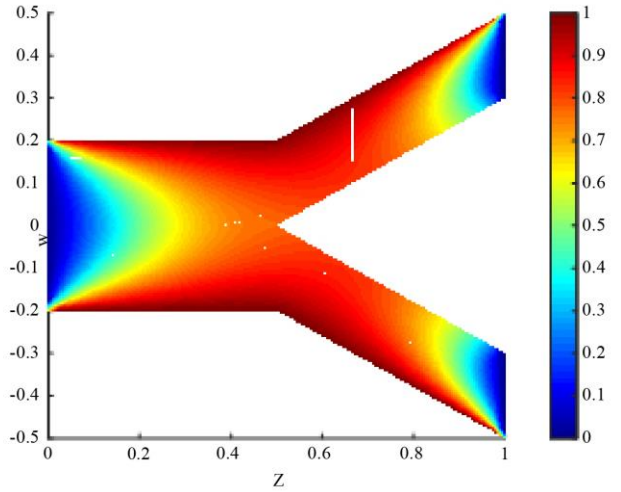

Fig. 13 CNT Deflection for φ = 60º

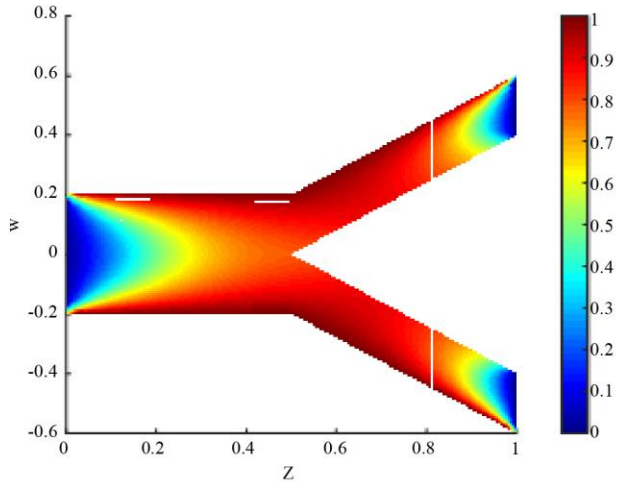

Fig. 14 CNT Deflection for φ = 75º

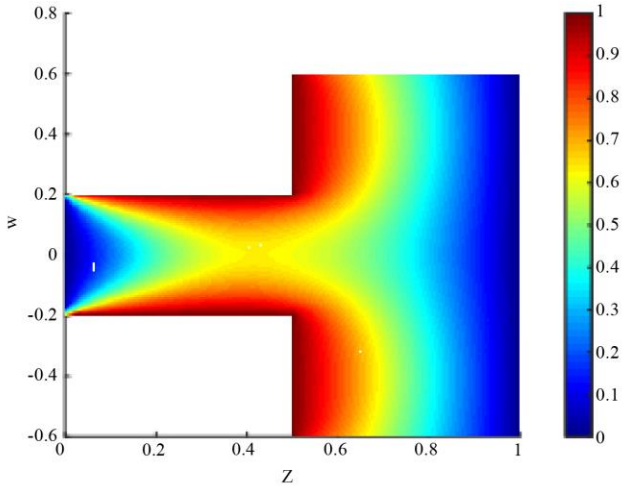

Fig. 15 CNT Deflection for φ = 90º

4.4. Visualization of CNT Dynamic Response for Different Downstream Angles with the Magnetic Field

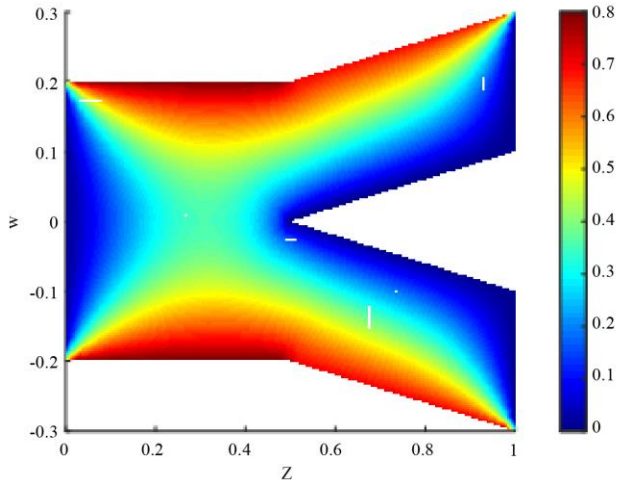

Fig. 16 CNT Deflection for φ = 0º

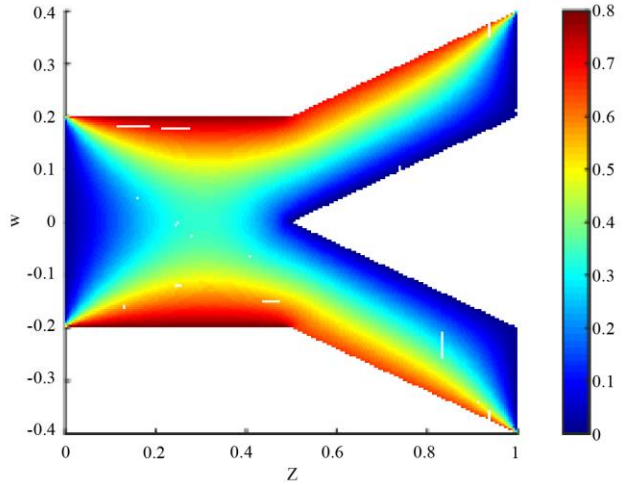

Fig. 17 CNT Deflection for φ = 30º

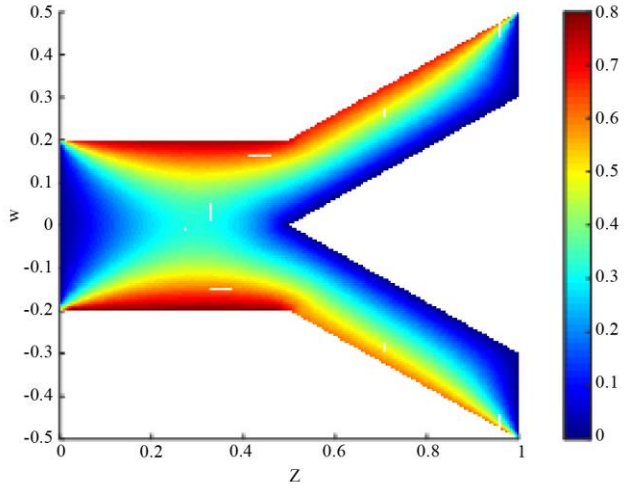

Fig. 18 CNT Deflection for φ = 45º

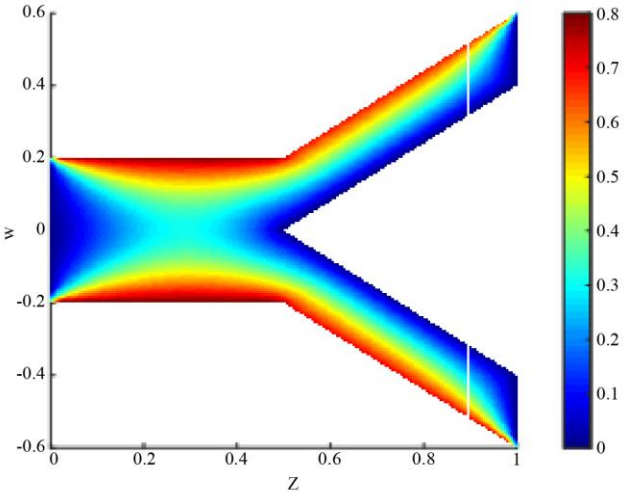

Fig. 19 CNT Deflection for φ = 60º

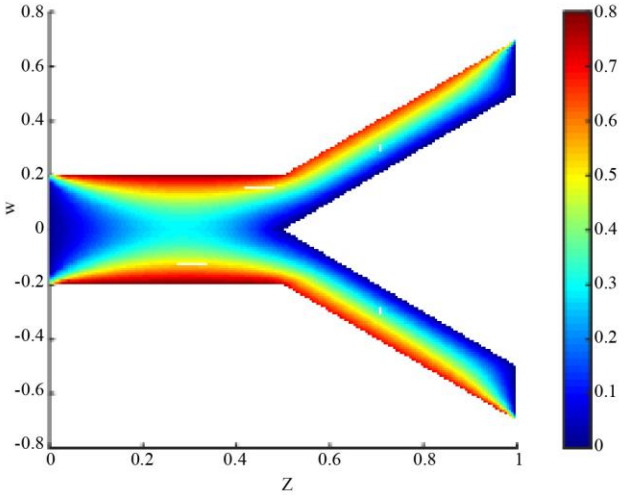

Fig. 20 CNT Deflection for φ = 75º

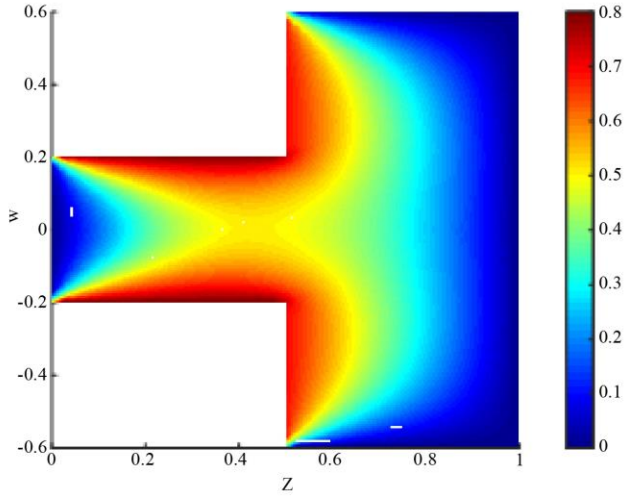

Fig. 21 CNT Deflection for φ = 90º

Figures 10-15 and figures 16-21 illustrate the visualization of CNT dynamic response for different downstream angles with and without magnetic fields. Flow-induced vibration without magnetic field results in a large deflection at the downstream joint. This is not desired in design as it automatically reduces the nanotube stability when the vibrating system is excited unto bifurcation and even flutter levels. The colour bars presented alongside the simulation solutions obtained after using the imposed conditions in the PDE-tool software help visualise the displacement at different nanotube points. This vibration displacement was noticed to be higher for weak or negligible magnetic fields domain. This increasing amplitude attributed to joints downstream is dampened by about 20 percent with the inclusion of a magnetic field. Furthermore, it was noticed that as the branched angle increases, the system loses its stability. This consequently enforces the need to ignore or limit the use of Tee nano-junctions for practical applications except for cases where a significant amount of magnetic field is present.

4.4. Verifications and Validations of Present Work

This section presents validations and verifications for the newly developed flow-induced nonlinear vibration models. A table of results is then prepared to visualize the novelty in the present study and how the developed models in the present study are reduced to the level of some already published works.

4.5. Verification with the Work of Wang et al. (2015)

Wang et al. (2015) analyzed the free vibration of fluid-conveying SWCNT under multi-physics fields (Figure 4.124). In order to establish a comparison, the coupled flow-induced vibration models in this study are reduced to the level of the research work carried out by Wang et al. (2015). The impact of the Magnetic field on the stability of the SWCNT is then compared with the present study.

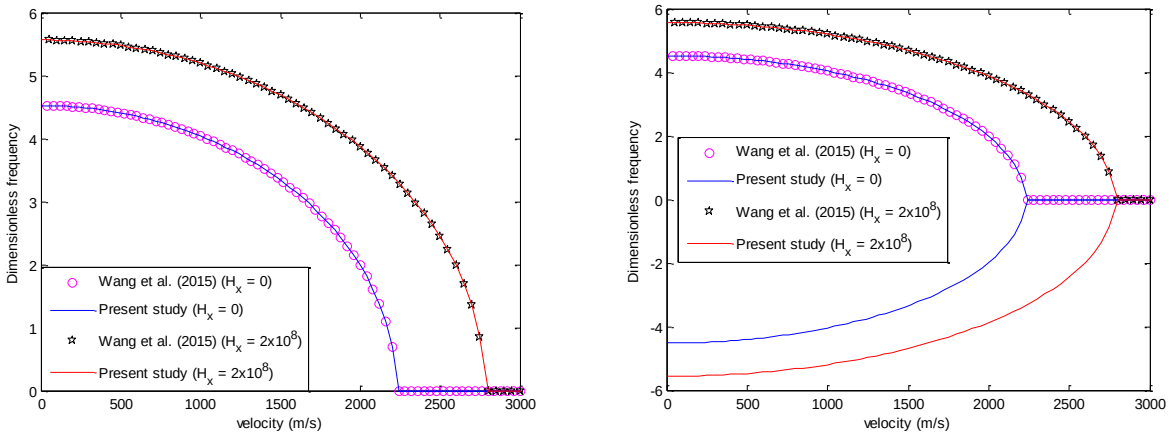

(a) **(b)**

Fig. 22 (a - b). Comparison of the present work with that of Wang et al. (2015)

4.6. Validation using the Work of Filiz and Aydogdu (2010)

On reducing the coupled flow-induced vibration model in the present study to that of axial vibration of carbon nanotube (Figure 23) using nonlocal elasticity, the Filiz and Aydogdu (2010) SWCNT model is recovered. The obtained relationship for the SWCNT amplitude and length, as well as frequency parameters and mode numbers, are then used for validation, as depicted in Figure 24 and Table 2, respectively.

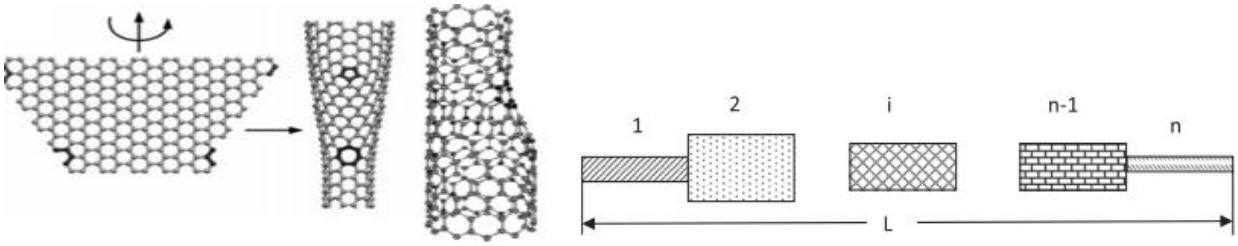

(a) **(b)**

Fig. 23 (a - b). Schematic of the SWCNT considered by Filiz and Aydogdu (2010)

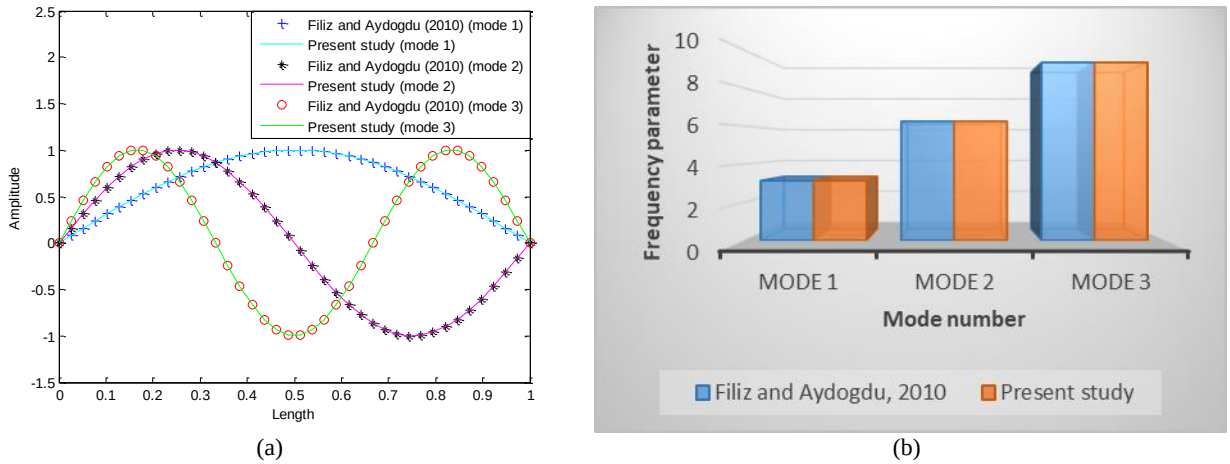

(a) (b)

Fig. 24 (a - b). Comparison of the present study with the work of Filiz and Aydogdu (2010)

Table. 2 Comparison of the present study with the work of Filiz and Aydogdu (2010)

	Frequency parameter	
	Filiz and Aydogdu (2010)	**Present study**
Mode 1	3.132	3.133
Mode 2	6.245	6.246
Mode 3	9.331	9.333

5. Conclusion

This work scrutinizes the non-linear magneto-mechanical longitudinal and transverse vibrations and stability analyses of different branched carbon nanotubes transporting viscous fluid and inserted in a two-parameter foundation in a Magnetic environment via Euler-Bernoulli, Hamilton variation and nonlocal elasticity theories. Equation of motions was obtained for coupled vibration models with flow velocity, deformation, thermal and pressure terms. The resulting systems of coupled PDEs were elucidated using an appropriate numerical scheme. The developed numerical solutions are used for parametric studies. Furthermore, the natural frequency obtained in the present study is reduced to the level of Wang *et al.* (2015) and that of Filiz and Aydogdu (2010), with a good agreement established. The present study is envisioned to progress the applicability of CNT for mechanical, electrical and structural systems, such as in the design and optimization of nano pumps, nano-injectors, nanotransistors, diodes and switch circuits due to its tremendous properties.

Nomenclatures

u	axial displacement component	Kn	Knudsen number
w	transverse displacement component	E	Modulus of elasticity
B	2D magnetic field	C_p	Specific heat capacity
k	Thermal conductivity	U	fluid velocity
∇	Gradient	n	Modal number
M_x^{CNT}	moment on SWCNT	G, k_w	shear modulus, Winkler foundation
I^{CNT}	moment of area of CNT	ρ_j^f	the density of the fluid in the junction
ρ_f	fluid density	$e_o a$	non local parameter
$\dot{w}$	derivative with respect to time	w''	derivative with respect to the spatial variable
M	Mass	C	Damper
K	Stiffness	L	CNT length
B	Magnetic field	Γ_{ij}	Frequency function
Λ_i	Eigenvectors	P, A	Pressure, Area
r	Radial component	z, t	Axial component, time
δ	variational parameter	ϕ	downstream angle
ϕ_{np}	nanoparticle volume fraction	q	Qualitative displacement function
U_c	Critical fluid velocity	U_s	Divergent fluid velocity

Funding Statement

The Authors received no grant or financial support for the publication of this manuscript.

Acknowledgments

The Authors appreciate the University of Lagos, Faculty of Engineering, for providing data and environment.

References

[1] R. Ansari, M. Hemmatnezhad, and J. Rezapour, "The Thermal Effect on Nonlinear Oscillations of Carbon Nanotubes with Arbitrary Boundary Conditions," *Current Applied Physics*, vol. 11, no. 3, pp. 692–697, 2011. [CrossRef] [Google Scholar] [Publisher Link]

[2] Hassan Askari, Ebrahim Esmailzadeh, and Davood Younesian, "Nonlinear Forced Vibration of Carbon Nanotubes Considering Thermal Effects," *26th Conference on Mechanical Vibration and Noise*, vol. 8, pp. 10-21, 2015. [CrossRef] [Google Scholar] [Publisher Link]

[3] Abdelkadir Belhadj, Abdelkrim Boukhalfa, and Sid Ahmed Belalia, "Carbon Nanotube Structure Vibration Based on Nonlocal Elasticity," *Journal of Modern Materials*, vol. 3, no. 1, pp. 9-13, 2017. [CrossRef] [Google Scholar] [Publisher Link].

[4] Bijan Mohamadi, S.Ali Eftekhari, and Davood Toghraie, "Numerical Investigation of Nonlinear Vibration Analysis for Triple-Walled Carbon Nanotubes Conveying Viscous Fluid," *International Journal of Numerical Methods for Heat & Fluid Flow*, vol. 30, no. 4, pp. 1-36, 2019. [CrossRef] [Google Scholar] [Publisher Link]

[5] L.A. Chernozatonskii, "Carbon Nanotubes Connectors and Planar Jungle Gyms," *Physics Letters A*, vol. 172, no. 3, pp. 173–176, 1992. [CrossRef] [Google Scholar] [Publisher Link]

[6] M. A. Eltaher, and N. Mohamed, "Free Vibration Analysis of a Perfect and Imperfect Single Walled Carbon Nanotube under Pre-Buckling and Post-Buckling Load," *Applied Mathematics and Computation*, vol. 382, 2020. [Google Scholar]

[7] Satyabrata Podder, Paulam Deep Paul, and Arunabha Chanda, "The Effect of the Magnetic Field of High Intensities on Velocity Profiles of Slip Driven Non-Newtonian Fluid Flow through the Circular, Straight Microchannel," *International Journal of Engineering Trends and Technology*, vol. 70, no. 4, pp. 383-388, 2022. [CrossRef] [Google Scholar] [Publisher Link]

[8] Feng Liang, and Yong Su, "Stability Analysis of a Single-Walled Carbon Nanotube Conveying Pulsating and Viscous Fluid with Nonlocal Effect," *Applied Mathematical Modelling*, vol. 37, no. 10-11, pp. 6821-6828, 2013. [CrossRef] [Google Scholar] [Publisher Link]

[9] Vincent O. S. Olunloyo, Charles A. Osheku, and Adekunle O. Adelaja, "On The Mechanics of Pipe Walking: Case of a Buried Pipeline," *29th International Conference on Offshore Mechanics and Arctic Engineering*, pp. 143-164, 2010.[CrossRef] [Google Scholar] [Publisher Link]

[10] Masoud Rafiei, Saeed Reza Mohebpour, and Farhang Daneshmand, "Small-Scale Effect on the Vibration of Non Uniform Carbon Nanotubes Conveying Fluid and Embedded in Viscoelastic Medium," *Physica E: Low Dimensional Systems and Nanostructures*, vol. 44, no. 7-8, pp. 1372–1379, 2012. [CrossRef] [Google Scholar] [Publisher Link]

[11] Mesut Şimşek, "Nonlocal Effects in the Forced Vibration of an Elastically Connected Double-Carbon Nanotube System under a Moving Nanoparticle," *Computational Materials Science*, vol. 50, no. 7, pp. 2112–2123, 2011. [CrossRef] [Google Scholar] [Publisher Link]

[12] M. G. Sobamowo et al., "Coupled Effects of Magnetic Field, Number of Walls, Geometric Imperfection, Temperature Change, and Boundary Conditions on Nonlocal Nonlinear Vibration of Carbon Nanotubes Resting on Elastic Foundations," *Forces in Mechanics*, vol. 3, pp. 1-41, 2021. [CrossRef] [Google Scholar] [Publisher Link]

[13] M. Terrones et al., "Molecular Junctions by Joining Single-Walled Carbon Nanotubes," *Physical Review Letters*, vol. 89, 2002. [CrossRef] [Google Scholar] [Publisher Link]

[14] Bo Wang et al., "Free vibration of Wavy Single-Walled Fluid-Conveying Carbon Nanotubes in multi-physics fields," *Applied Mathematical Modelling*, vol. 39, no. 22, pp. 6780-6792, 2015. [CrossRef] [Google Scholar] [Publisher Link]

[15] A.A. Yinusa, M.G. Sobamowo, and A.O. Adelaja, "Thermal Analysis of Nanofluidic Flow Through Multi-Walled Carbon Nanotubes Subjected to Perfectly and Inperfectly Bonded Wall Conditions," *Chemical Thermodynamics and Thermal Analysis*, vol. 5, 2022. [CrossRef] [Google Scholar] [Publisher Link]

[16] A.A. Yinusa, and M.G. Sobamowo, "Mechanics of Nonlinear Internal Flow Induced Vibration And Stability Analysis of a Pre-Tensioned SWCNT using classical DTM with CAT and SAT after Treatment Techniques," *Forces in Mechanics*, vol. 7, 2022. [CrossRef] [Google Scholar] [Publisher Link]

[17] P. Seshu Mani, S. Vijaya Bhaskara Rao, "Effect of Magnetic Field on Viscosity and Excess Viscosity of Three Liquid Mixtures," *SSRG International Journal of Electrical and Electronics Engineering*, vol. 4, no. 7, pp. 10-18, 2017. [CrossRef] [Publisher Link]

[18] A.A. Yinusa, M.G. Sobamowo, and A.O. Adelaja, "Flow Induced Bifurcation and Phase-Plane Stability Analysis of Branched Nanotubes Resting on Two Parameter Foundation in A Magnetic Environment," *Partial Differential Equations in Applied Mathematics*, vol. 5, 2022. [CrossRef] [Google Scholar] [Publisher Link]

[19] A.A. Yinusa, and M.G. Sobamowo, "Thermal Instability and Dynamic Response Analysis of a Tensioned Carbon Nanotube Under Moving Uniformly Distributed External Pressure," *Nano Material Science*, vol. 3, no. 1, pp. 75-88, 2021. [CrossRef] [Google Scholar] [Publisher Link]

[20] A.A. Yinusa, M.G. Sobamowo, and A.O. Adelaja, "Nonlinear Vibration Analysis of an Embedded Branched Nanofluid-Conveying Carbon Nanotube: Influences of Downstream Angle, Temperature Change and Two Dimensional External Magnetic Field," *Nano Material Science*, vol. 2, no. 4, pp. 323-332, 2020. [CrossRef] [Google Scholar] [Publisher Link]

[21] A. Ahmed Yinusa, and M. Gbeminiyi Sobamowo, "Analysis of Dynamic Behaviour of a Tensioned Carbon Nanotube in Thermal and Pressurized Environments," *Karbala International Journal of Modern Science*, vol. 5, no. 1, pp. 1-11, 2019. [CrossRef] [Google Scholar] [Publisher Link]

[22] A.A. Yinusa, M.G. Sobamowo, and A.O. Adelaja, "Detrmination of the Dynamic Shearing Force and Bending Moment of a Tension Single-Walled Carbon Nanotube Subjected to a Uniformly Distributed External Pressure," *Engineering and Applied Science Letters*, vol. 3, no. 2, pp. 40-52, 2019. [CrossRef] [Google Scholar] [Publisher Link]

[23] Haruna Abubakar, Adisa A. Bello, and Robinson I. Ejilah, "Development of Mathematical Model of a Utility Boiler Based on Energy and Exergy Analysis," *SSRG International Journal of Thermal Engineering*, vol. 6, no. 1, pp. 1-10, 2020. [CrossRef] [Google Scholar] [Publisher Link]

[24] S. Sami, "Prediction of Behavior of Thermal Storage, PV-Thermal Solar Collector with Nanofluids and Phase Change Material," *SSRG International Journal of Thermal Engineering*, vol. 6, no. 1, pp. 11-27, 2020. [CrossRef] [Google Scholar] [Publisher Link]

[25] Simon Taylor et al., "Diesel Engine Waste Heat Harnessing ORC," *SSRG International Journal of Thermal Engineering*, vol. 6, no. 1, pp. 29-35, 2020. [CrossRef] [Google Scholar] [Publisher Link]

[26] Yash Hareshbhai Beladiya, "Performance Improvement of Biomass Cookstove with the Help of Swirl Inducement," *SSRG International Journal of Thermal Engineering*, vol. 8, no. 2, pp. 1-6, 2022. [CrossRef] [Google Scholar] [Publisher Link]

[27] S. Sami, "The Behavior of Magnetized PV-Th Integrated Organic Rankine Cycle ORC with Cooling Capabilities," *SSRG International Journal of Thermal Engineering*, vol. 8, no. 1, pp. 1-12, 2022. [CrossRef] [Google Scholar] [Publisher Link]